Displacement Induced Torsion in Structures

M. Masoudi
ROSE Programme, UME School, IUSS Pavia, Italy

P. Gülkan
Çankaya University, Ankara, Turkey

A. Dazio
EUCENTRE, Pavia, Italy

SUMMARY:
Satisfying the equations of motion in the deformed configuration leads to actions that inherently contain secondary effects. Similar to the product of vertical loads and lateral displacements which leads to the P−Δ effect in structures, lateral displacements may cause significant secondary torsion due to the presence of lateral loads. A simple finite-element formulation is presented in the paper to capture this effect. This formulation is verified by means of the Corotational approach and the updated Lagrangian formulation for acceptable drift limits in structural engineering practice. A simple single-story structure and a 7-story RC and steel structures with no predefined mass eccentricity are subjected to an ensemble of bi-axial ground motions recorded on different soil conditions to demonstrate secondary effects. The paper shows that when the period of the structure is not identical in the two horizontal directions secondary torsion is important and may result in significant torsional amplification.

Keywords: torsional response, accidental eccentricity, geometric nonlinearity, second order effects

1. INTRODUCTION

Generally, the geometric-stiffness property represents the tendency toward buckling induced in a structure by axially directed load components. Thus it depends not only on the configuration of the structure but also on its condition of loading (Clough and Penzien, 1993). This concept has been developed further here for 3D beam elements by considering other nodal actions. In static problems the nodal actions are constant and consequently the geometric-stiffness property is time invariant. However, during dynamic loading the nodal actions especially horizontal actions vary significantly with time; so, the geometric-stiffness should be updated with time for numerical solutions.

The finite-element method can be used to obtain a higher order approximation of geometric stiffness. There are two well-documented and robust approaches to consider all geometric nonlinear effects with high accuracy for 3D beam elements. The first one is the Corotational approach (Crisfield, 1991, Crisfield, 1997) that refers to the idea that the local element frame continuously rotates with the element and the tangent stiffness matrix remains intact during the analysis procedure. This approach is applicable to large deformation but small-strain problems. The second one is the total or updated Lagrangian formulation derived from the principles of continuum mechanics (Bathe and Bolourchi, 1979) and involves approximate interpolation functions and numerical integration. This approach can be used efficiently for large displacement and large rotation analysis. However, it requires multiple elements per member to achieve accuracy. These two methods have been implemented in several commercial software packages like SAP2000 (CSI, 2011) that use updated Lagrangian formulation as well as research oriented and open source programs like Opensees (McKenna et al., 2010) that use the Corotational approach with some modifications (De Souza, 2000). A large number of publications are available in the literature which present modified or special purpose methods and solution techniques based on the Corotational and Lagrangian formulations.

Usually, the mathematical formulation for considering geometric nonlinearity is heavy and the physical meaning of the derived relationships may be lost in the complexity of the mathematical approaches. This paper presents a simple formulation to handle secondary effects efficiently in a 3D beam element for structural engineering purposes. By using the derived formulation the effect of secondary effects on the torsional response of single-story structures has been evaluated. Furthermore, to identify secondary torsional effects in multi-story structures, a 7-story RC and steel case study buildings have been analysed by a software (SeismoSoft, 2010) which uses the Corotational formulation to consider geometric nonlinearities.

2. EXTENDED GEOMETRIC-STIFFNESS FOR 3D BEAM ELEMENTS

The deformed shape of a uniform 2D beam subjected to nodal displacements can be expressed by a linear combination of cubic Hermitian polynomials. For a 3D beam element, the deformed shape can be expressed in terms of the projected deformed shapes on two perpendicular planes passing through the element longitudinal axis. The projected shapes can be approximated by cubic Hermitian shape functions to derive a solid form of geometric stiffness matrix. This is in agreement to what has been done in the past (Clough and Penzien, 1993) to obtain the consistent geometric stiffness matrix which allow considering the effect of axial load on the deformed shape, i.e. P–Δ effects. When an element undergoes inelastic deformations, the deformed shape deviates from the cubic shape and gets closer to a linear shape. However, it can be shown that the results are not sensitive to the chosen shape function.

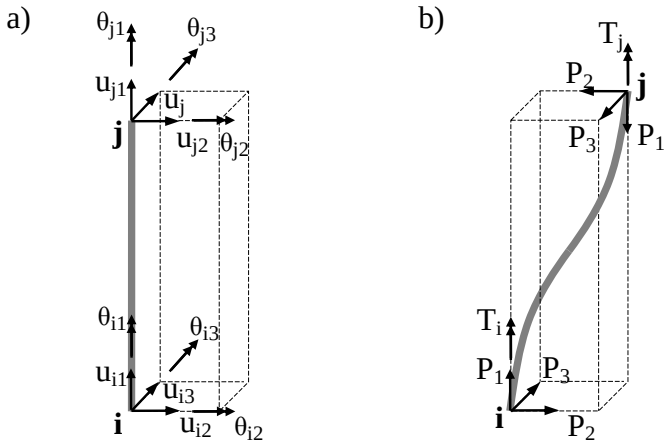

Figure 2.1. Degrees of freedom (a) and nodal actions causing secondary effects (b).

A 3D beam element with its local coordinate system, its degrees of freedom and its nodal actions is shown in Fig. 2.1. The main key in considering second order effects is to identify which nodal actions generate other displacements or rotations in addition to their primary effects. It is clear that moments acting about axes 2 and 3 cannot produce any second order effect. Only the actions which are capable of producing second order effects are shown in Fig. 2.1. The cubic interpolation functions can be expressed as:

$$\Psi_{it}(x) = 1 - \frac{3}{L^2}x^2 + \frac{2}{L}x^3 \tag{2.1}$$

$$\Psi_{ir}(x) = x\left(1 - \frac{x}{L}\right)^2 \tag{2.2}$$

$$\Psi_{jt}(x) = \frac{3}{L^2}x^2 - \frac{2}{L}x^3 \tag{2.3}$$

$$\Psi_{jr}(x) = \frac{x^2}{L}\left(\frac{x}{L} - 1\right) \tag{2.4}$$

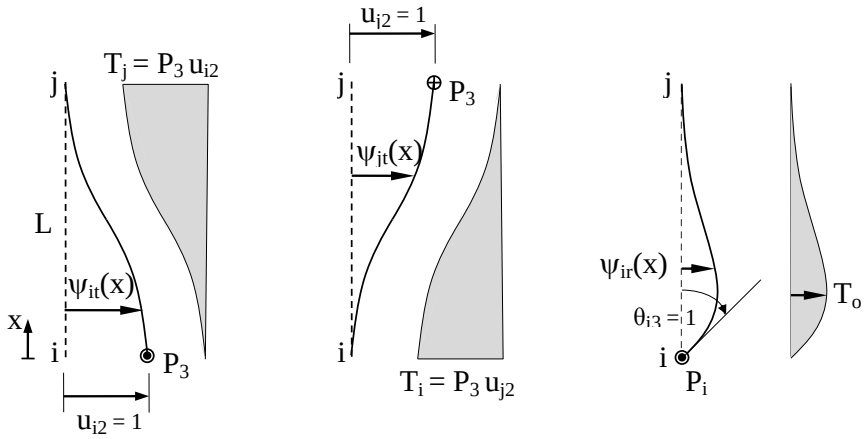

Figure 2.2. Beam deflections due to unit nodal displacement.

where Ψ_{it} and Ψ_{ir} are translational and rotational shape functions for node *i*, respectively. They are shown in Fig. 2.2 for the 1-2 local coordinate plane. The shown second order torsional moment diagram is one component of the resultant second order torsional diagram produced by the lateral nodal actions and the deviation of the deflected shape from the original configuration. The nonlinear second order torsion diagram causes a nonlinear distribution of angle of twist along the element length that can be calculated by the following relationships when u_{j2}=1.

$$\mathrm{d}\theta_{j1/i}(x) = -\frac{P_3\left(1-\Psi_{jt}(x)\right)}{GJ}\mathrm{d}x \tag{2.5}$$

$$\theta_{j1/i} = -\frac{P_3}{GJ}\int_0^L \Psi_{it}(x)\,\mathrm{d}x = -\frac{P_3 L}{2GJ} \tag{2.6}$$

where $\theta_{j1/i}$ is the angle of twist at node *j* with respect to node *i*. In order to have zero torsional displacement at node j, a torsional moment equal to $-\theta_{j1/i}GJ/L$ needs to be applied. Thus, the corresponding geometric-stiffness influence coefficient is $P_3/2$.
Furthermore, this second order torsion induced by P_3 and u_{j2} can produce a negligible third order displacement in the *j*3-direction equal to:

$$\mathrm{d}u_{j3}(x) = u_{j2}\left(1-\Psi_{jt}(x)\right)\mathrm{d}\theta_{j1/i}(x) = \frac{P_3 u_{j2}^2 \Psi_{it}^2(x)}{GJ}\mathrm{d}x \tag{2.7}$$

It is evident that the third order effects induced by the component nodal actions and displacements cannot be superimposed because they are proportional to the squares of the displacement.
In structural engineering practice, rotations and axial deformation of members are relatively small. Furthermore, nodal displacements are limited to certain values according to the desired performance level. In contrast to the Corotational and Lagrangian formulations, here it is assumed that axial deformations are negligible and rotations are small enough to be treated as a vector quantity.
The geometric-stiffness influence coefficients can be calculated by satisfying equilibrium and compatibility equations in the deformed configuration corresponding to the application of a unit displacement at the desired degree of freedom. This can alternatively be achieved by using the principle of virtual displacements. Detailed information on the derivation of the geometric-stiffness property can be found in (Masoudi, 2012). The extended geometric-stiffness matrix, $\mathbf{k}_G$, may be expressed as:

$$
\begin{array}{c|cccccccccc}
 & u_{i2} & u_{j2} & \theta_{i3} & \theta_{j3} & \theta_{i1} & u_{i3} & u_{j3} & \theta_{i2} & \theta_{j2} & \theta_{j1} \\
\hline
u_{i2} & -\frac{6P_1}{5L} & \frac{6P_1}{5L} & -\frac{P_1}{10} & -\frac{P_1}{10} & 0 & \frac{6EI_3}{GJ}\frac{T_i}{L^2} & -\frac{6EI_3}{GJ}\frac{T_j}{L^2} & \frac{EI_3}{GJ}\frac{T_i}{L} & -\frac{EI_3}{GJ}\frac{T_j}{L} & 0 \\
u_{j2} & \frac{6P_1}{5L} & -\frac{6P_1}{5L} & \frac{P_1}{10} & \frac{P_1}{10} & 0 & -\frac{6EI_3}{GJ}\frac{T_i}{L^2} & \frac{6EI_3}{GJ}\frac{T_j}{L^2} & -\frac{EI_3}{GJ}\frac{T_i}{L} & \frac{EI_3}{GJ}\frac{T_j}{L} & 0 \\
\theta_{i3} & -\frac{P_1}{10} & \frac{P_1}{10} & -\frac{2P_1L}{15} & \frac{P_1L}{30} & 0 & \frac{3EI_3}{GJ}\frac{T_i}{L} & -\frac{3EI_3}{GJ}\frac{T_j}{L} & -\frac{EI_3}{2GJ}T_i & \frac{EI_3}{GJ}\frac{T_j}{L} & 0 \\
\theta_{j3} & -\frac{P_1}{10} & \frac{P_1}{10} & \frac{P_1L}{30} & -\frac{2P_1L}{15} & 0 & \frac{3EI_3}{GJ}\frac{T_i}{L} & -\frac{3EI_3}{GJ}\frac{T_j}{L} & -\frac{EI_3}{2GJ}T_i & \frac{EI_3}{GJ}\frac{T_j}{L} & 0 \\
\theta_{i1} & -\frac{P_3}{2} & \frac{P_3}{2} & \frac{P_3L}{12} & \frac{P_3L}{12} & 0 & \frac{P_2}{2} & -\frac{P_2}{2} & \frac{P_2L}{12} & \frac{P_2L}{12} & 0 \\
u_{i3} & -\frac{6EI_2}{GJ}\frac{T_i}{L^2} & \frac{6EI_2}{GJ}\frac{T_j}{L^2} & \frac{EI_2}{GJ}\frac{T_i}{L} & -\frac{EI_2}{GJ}\frac{T_j}{L} & 0 & -\frac{6P_1}{5L} & \frac{6P_1}{5L} & \frac{P_1}{10} & \frac{P_1}{10} & 0 \\
u_{j3} & \frac{6EI_2}{GJ}\frac{T_i}{L^2} & -\frac{6EI_2}{GJ}\frac{T_j}{L^2} & -\frac{EI_2}{GJ}\frac{T_i}{L} & \frac{EI_2}{GJ}\frac{T_j}{L} & 0 & \frac{6P_1}{5L} & -\frac{6P_1}{5L} & -\frac{P_1}{10} & -\frac{P_1}{10} & 0 \\
\theta_{i2} & \frac{3EI_2}{GJ}\frac{T_i}{L} & -\frac{3EI_2}{GJ}\frac{T_j}{L} & -\frac{EI_2}{2GJ}T_i & \frac{EI_2}{2GJ}T_j & 0 & \frac{P_1}{10} & -\frac{P_1}{10} & -\frac{2P_1L}{15} & \frac{P_1L}{30} & 0 \\
\theta_{j2} & \frac{3EI_2}{GJ}\frac{T_i}{L} & -\frac{3EI_2}{GJ}\frac{T_j}{L} & -\frac{EI_2}{2GJ}T_i & \frac{EI_2}{2GJ}T_j & 0 & \frac{P_1}{10} & -\frac{P_1}{10} & \frac{P_1L}{30} & -\frac{2P_1L}{15} & 0 \\
\theta_{j1} & -\frac{P_3}{2} & \frac{P_3}{2} & -\frac{P_3L}{12} & -\frac{P_3L}{12} & 0 & \frac{P_2}{2} & -\frac{P_2}{2} & -\frac{P_2L}{12} & -\frac{P_2L}{12} & 0
\end{array}
\tag{2.8}
$$

To avoid confusion related to the sign convention, in contrast to the traditional way of expressing the total stiffness matrix, $\mathbf{k}_t$, the geometric-stiffness matrix is added to the stiffness matrix rather than subtracted.

$$\mathbf{k}_t = \mathbf{k} + \mathbf{k}_G \tag{2.9}$$

For a double cantilever element this formulation is in very good agreement with both the Corotational and the Lagrangian approach up to 4% drift.

3. RESPONSE OF SINGLE-STORY STRUCTURES

The equation of motion of the symmetric single-story 3D structure shown in Fig. 3.1 can be expressed as:

$$\mathbf{m}\ddot{\mathbf{u}} + \mathbf{k}_t\mathbf{u} = \mathbf{F} \tag{3.1}$$

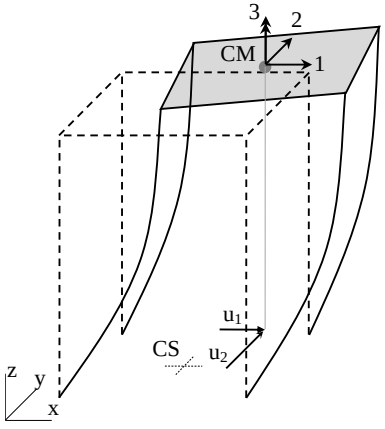

Figure 3.1. A symmetric single-story structure subjected to a bi-axial dynamic loading.

where **F** is the vector of external forces and in case of a bi-axial excitation is equal to:

$$\mathbf{F} \equiv \left\{F_1(t), F_2(t), 0\right\}^T \tag{3.2}$$

The frame is represented by a system with one rotational and two horizontal degrees of freedom. The system is nominally symmetric and has no structural or accidental mass or stiffness eccentricity. In order to consider second-order effects caused by member forces, the stiffness matrix should be formed according to all nodal forces (system reactions) in the deformed configuration which is equal to:

$$\bar{\mathbf{F}} \equiv \mathbf{k}_t \mathbf{u} = \mathbf{F} - \mathbf{m}\ddot{\mathbf{u}} \tag{3.3}$$

By using the condensed form of the geometric-stiffness matrix given by Eqn. 2.8 and substituting the relevant lateral and torsional stiffness of the system instead of *EI* and *GJ*, the total stiffness matrix can be expressed in the following form:

$$\mathbf{k}_t = \begin{bmatrix} k_1 & \dfrac{k_1}{2k_3}\bar{F}_3 & 0 \\ -\dfrac{k_2}{2k_3}\bar{F}_3 & k_2 & 0 \\ -\dfrac{\bar{F}_2}{2} & \dfrac{\bar{F}_1}{2} & k_3 \end{bmatrix} \tag{3.4}$$

where, k_1, k_2 and k_3 are translational and rotational stiffness influence coefficients and $\bar{F}_1, \bar{F}_2$ and $\bar{F}_3$ are elements of $\bar{\mathbf{F}}$. Initially, the system features three uncoupled equations of motion and the stiffness matrix has no off-diagonal elements. However, as the lateral forces build up, off-diagonal terms make the system slightly coupled. The frequency equation of the system yields the modal properties of the frame.

$$\left|\mathbf{k}_t - \omega^2 \mathbf{m}\right| = 0 \tag{3.5}$$

$$\left(k_1 - m\omega^2\right)\left(k_2 - m\omega^2\right)\left(k_3 - m\omega^2\right) + \frac{k_1 k_2}{4k_3^2}\bar{F}_3^2\left(k_3 - m\omega^2\right) = 0 \tag{3.6}$$

It is evident that the torsional frequency of the system is not altered by coupling effects because k_3/m is a root of the frequency equation. Thus, Eqn. 3.6 can be reduced to:

$$\left(k_1 - m\omega^2\right)\left(k_2 - m\omega^2\right) + \frac{k_1 k_2}{4k_3^2}\bar{F}_3^2 = 0 \tag{3.7}$$

According to Eqn 3.7, the lateral natural frequencies of the system are time variant and depend on the magnitude of the torsional reaction. However, for nominally symmetric structures the order of magnitude of secondary torsion is expected to be smaller than other forces. Therefore, it can be assumed that the free vibration frequencies in both horizontal directions remains unchanged regardless the secondary effects.

It can be shown that if the undamped system is subjected to a biaxial set of harmonic excitations with ϖ_1 and ϖ_2 frequencies, then the approximate steady-state torsional response is equal to (Masoudi, 2012):

$$u_3(t) = B_1 B_2 \left(\frac{\omega_2^2 - \omega_1^2}{4r^2 \omega_3^2} \right) \left(\frac{\cos(\bar{\omega}_1 - \bar{\omega}_2)t - \cos\omega_3 t}{1 - \left(\frac{\bar{\omega}_1 - \bar{\omega}_2}{\omega_3} \right)^2} - \frac{\cos(\bar{\omega}_1 + \bar{\omega}_2)t - \cos\omega_3 t}{1 - \left(\frac{\bar{\omega}_1 + \bar{\omega}_2}{\omega_3} \right)^2} \right) \tag{3.8}$$

where ω_1, ω_2 and ω_3 are lateral frequencies and the torsional frequency of the system, respectively and r is the mass radius of gyration. B_1 and B_2 are the amplitudes of the uncoupled harmonic response in the lateral directions. It is clear that higher order harmonics, $\varpi_1 + \varpi_2$ and $\varpi_1 - \varpi_2$, appear in the torsional response due to second order effects. Fig 3.2 shows the displacement response of the four edges of a geometric-nonlinear symmetric system normalized to the displacement response of the same system without geometric nonlinearity. The lateral periods of the system are T_1 = 2s and T_2 = 1s and subjected to harmonic loads with periods of $\bar{T}_1$ = 1s and $\bar{T}_2$ = 4s, respectively, while the torsional period of the system is T_θ = 3s. The system has 5% damping with no predefined static eccentricity between the centre of mass (CM) and the centre of rigidity (CR). Interestingly, the system shows about 32% maximum amplification of the displacement solely due to second order effects. It is worth noting that this is a special case of very long period loading and torsionally very flexible system.

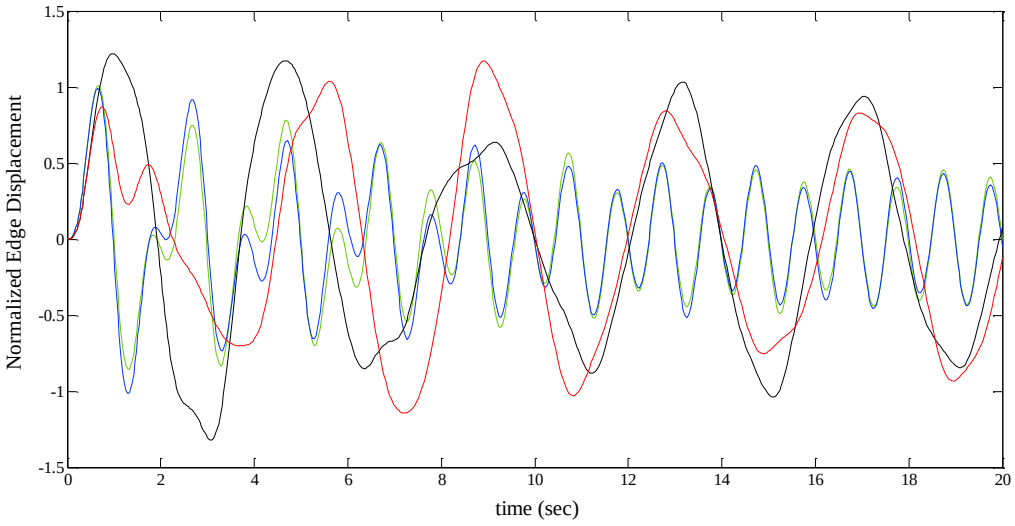

Figure 3.2. Normalized displacements of the four edges of a single-story system subjected to a bi-axial harmonic loading.

The aforementioned system shown in Fig. 3.1 has been subjected to an ensemble of 9 bi-axial earthquake ground motions on different soil conditions. In each earthquake both records are scaled by a same factor to limit the displacement response to 4% drift in the direction of the dominant component. The response of the system has been calculated for a wide range of T_2/T_1 ratios, i.e. the ratio between the lateral periods of the system, and T_1.

As a measure for the resulting torsion, the traditional definition of *equivalent static accidental eccentricity* (Newmark and Rosenblueth, 1971), e_d , in Eqn. 4.1 implicitly assumes that the peak values of base shear and base torsion occur simultaneously. This definition may cause a misconception that systems with identical lateral and torsional vibration periods show the largest torsional amplification (De la Llera and Chopra, 1994).

$$e_{d1} = \frac{T_{max}}{V_{2,max}} \quad , \qquad e_{d2} = \frac{T_{max}}{V_{1,max}} \tag{3.9}$$

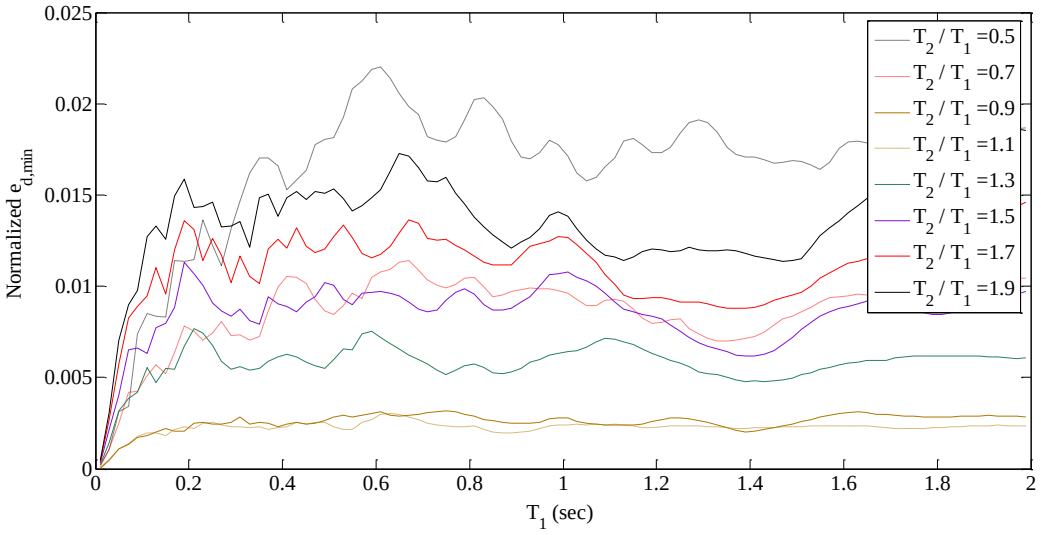

Figure 3.3. Average eccentricity spectra for single-story structures subjected to 45° rotated bi-axial records.

Average spectra for the minimum of e_{d1} and e_{d2} are plotted in Fig. 3.3. The eccentricities are normalized to the plan dimension of the building.

It is evident that when the ratio T_2/T_1 approaches unity the torsional response approaches zero. This can be proved mathematically that for symmetric single-story structures having a geometric-stiffness matrix like Eqn. 3.4 the torsional response is minimized when the lateral periods of the system are equal. For exactly the same dynamic loading in both lateral directions the torsional response is zero. In the case of a bi-axial static loading the angle of twist is always zero if the lateral stiffness in both directions is equal. However, in multi-story buildings the torsional response in the case of $T_2 = T_1$ is not necessarily zero (Masoudi, 2012). Furthermore, the shown spectra are not sensitive to the direction of earthquake attack (Masoudi, 2012).

It should be noted that the most realistic measure to compare torsional amplification in two models is the ratio between the displacements of the edges of the models. Based on this approach, second order effects generally cause a deamplification of the edge displacement in linear elastic structures because they soften the structure similar to the P−Δ effect and consequently they reduce the seismic demand. Nevertheless, there are special cases where second order torsion may significantly amplify the displacements of the edges like it has been shown in Fig 3.2.

However, in structures with both material and geometric nonlinearity the situation is different and second order torsion can amplify the edges demands when the system enters the inelastic range of response due to the material nonlinearity. This will be shown in the next section.

4. RESPONSE OF MULTY-STORY STRUCTURES: A CASE STUDY

A seven-story reinforced concrete (RC) building with a regular configuration has been considered as the case study. It is a simple symmetric 3D moment resisting frame. This structure is 22 meter high and features one 6 meter bay in both horizontal directions. This RC frame has been designed according to FEMA 450 (Building Seismic Safety Council (BSSC), 2004) and has been subjected to an ensemble of 8 earthquake ground motions. Fig. 4.1 shows the plan and elevation view of the case study building. In the case study, also a second building is considered. The second building is a 3D steel moment resisting structure which has exactly the same geometric configuration as the RC example.

Three computer models have been assembled for each building using SeismoStruct (SeismoSoft, 2010). The first one is a *linear elastic model* with a centric mass in all floors. The second one is a

linear elastic model with an eccentric mass in all floors which is an assumption commonly used for the analysis of such frames. A mass eccentricity equal to 5% of the plan dimension, i.e. 0.05×6 = 0.30m, is considered in both horizontal directions. De la Llera and Chopra (1994) states that the increase in building response resulting from accidental eccentricity varying among different stories is slightly (generally less than 10%) larger than the increase in building response computed using the same accidental eccentricity in all stories. Furthermore, it is common in practice to shift the centre of mass of all floors the same amount e_a in the same direction (De la Llera and Chopra, 1995). The third computer model is a *geometric-nonlinear* model with a centric mass in all floors. This model is assembled using elastic elements with uncoupled lumped plastic hinges at both ends. The uncoupled lumped plastic hinges do not consider the interaction between axial load and moment capacity to avoid any nonlinearity induced by strength-dependent stiffness.

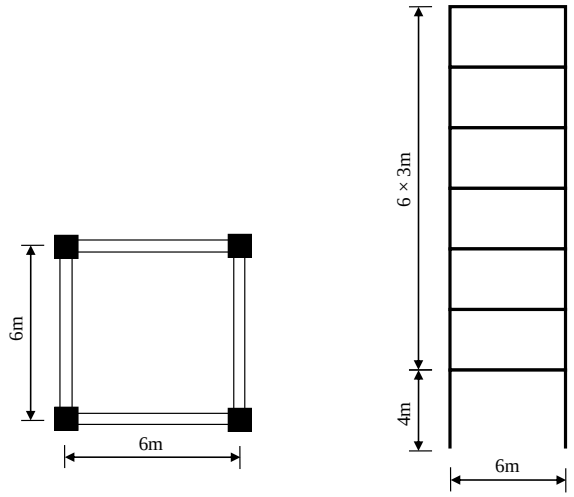

Figure 4.1. Plan and elevation of the case study building frame.

All models have been subjected to a set of eight bi-axial earthquake ground motions. In order to avoid any scaling procedure and use original records, the dominant components of all selected ground motions have spectral accelerations at short periods as well as at a period of one second that are very close to the considered design spectrum. The aim of the time history analyses is to evaluate effects of second order torsion on the seismic demand of this building frame compared with the outcome of the so-called "5% accidental eccentricity".

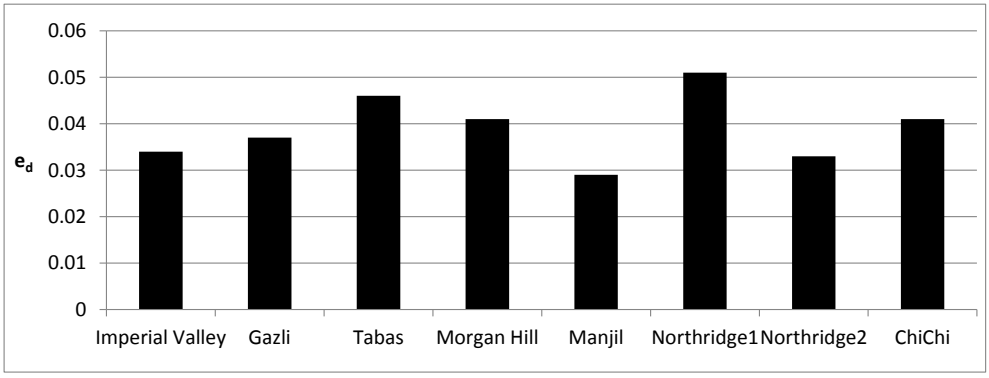

Figure 4.2. Equivalent static accidental eccentricity caused by second order effects in the 7-story RC building.

Fig. 4.2 shows the *equivalent static accidental eccentricity* e_d caused by second order effects in the 7-story RC building. The eccentricity e_d is calculated based on the maximum base shear in both horizontal directions. Thus, it gives a smaller e_d for the direction perpendicular to the dominant horizontal component. It is evident that in contrast to elastic single-story structures that show no second order torsion in case of equal lateral periods, in multi-story buildings the second order torsion

is significant even for identical modal properties in both lateral directions. This is a consequence of the interaction between material and geometric nonlinearities. Once the system enters the material inelastic range, then small second-order torsion can cause an unbalance between the vibratory properties of the lateral directions.

A more reasonable measure of the second order torsion is perhaps the maximum base column shear in the aforementioned three models. In Fig. 4.3 and Fig. 4.4 the maximum of the base column shear in the linear mass-eccentric as well as in the geometric-nonlinear model is normalized to the corresponding value in the mass-centric linear model. The results show that for both the RC and the steel building the second order torsion is capable of amplifying the shear demands up to 24 and 14%, respectively. The RC building is stiffer than the steel building, therefore it has to bear larger lateral loads and consequently the secondary torsion is more severe in the RC building. Furthermore, in some earthquakes the RC structure responds mainly elastically thus second order effects soften the structure and consequently cause deamplification of the base column shear.

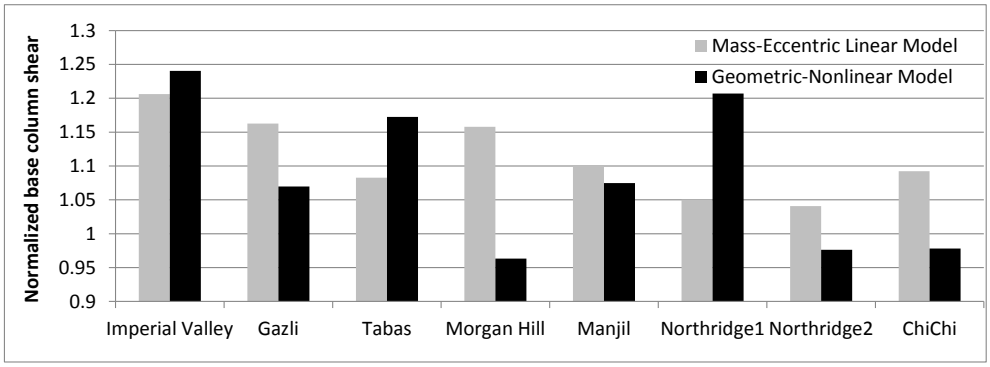

Figure 4.3. Maximums of the uneven normalized base column shear in the linear mass-eccentric and geometric nonlinear models of the 7-story RC building.

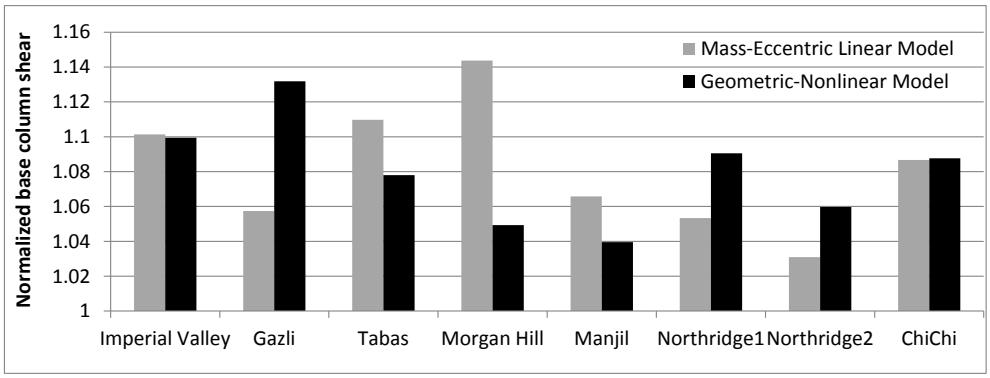

Figure 4.4. Maximums of the uneven normalized base column shear in the linear mass-eccentric and geometric nonlinear models of the 7-story steel building

5. CONCLUSIONS

A simple finite-element formulation based on the extension of the geometric-stiffness property has been developed. This formulation provides a physical understanding of second order effects at presence of all nodal actions. By means of the proposed formulation it is much easier and more straightforward to study the response of simple systems subjected to classical excitations like e.g. harmonic loading. This help understanding how the vibratory properties of a system may be affected by second order effects.

In single-story structures, based on the traditional definition of *equivalent static accidental*

eccentricity, second order effects may cause a torsional amplification about the order of magnitude of the code-specified eccentricity. However, in torsionally flexible structures the edge demands may be amplified even more significantly.

In multi-story structures second order torsion plays an important role because it can generate a larger amplification compared to linear mass-eccentric models which are commonly recommended by code provisions to account for accidental eccentricity. This could necessitate a re-evaluation of codified accidental eccentricity to account for this unforeseen source of accidental torsion.

REFERENCES

Bathe, K.-J. & Bolourchi, S. (1979). Large displacement analysis of three-dimensional beam structures. *International Journal for Numerical Methods in Engineering,* **14:7,** 961-986.

Building Seismic Safety Council (Bssc) (2004). *NEHRP Recommended Provisions for Seismic Regulations for New Buildings and Other Structures*, Washington, DC, USA, FEMA 450, National Institute of Building Sciences.

Clough, R.W. & Penzien, J. (1993). *Dynamics of Structures*, New York, USA, McGraw-Hill.

Crisfield, M.A. (1991). *Non-linear Finite Element Analysis of Solids and Structures*, Chichester ; New York, John Wiley & Sons.

Crisfield, M.A. (1997). *Non-linear Finite Element Analysis of Solids and Structures*, John Wiley & Sons.

CSI (2011). *CSI Analysis Reference Manual*, Berkeley, USA, Computers and Structures, Inc.

De La Llera, J.C. & Chopra, A.K. (1994). Using accidental eccentricity in code-specified static and dynamic analyses of buildings. *Earthquake Engineering & Structural Dynamics,* **23:9,** 947-967.

De La Llera, J.C. & Chopra, A.K. (1995). Estimation of accidental torsion effects for seismic design of buildings. *Journal of Structural Engineering-ASCE.,* **121:1,** 102-114.

De Souza, R.M. (2000). *Force-Based Finite Element for Large Displacement Inelastic Analsysis of Frames.* Ph.D. Dissertation, University of California at Berkeley.

Masoudi, M. (2012). *Secondary dynamic torsion in structural systems.* Ph.D. Dissertation, IUSS Pavia.

McKenna, F., McGann, C., Arduino, P. & Harmon, J. A. (2010). OpenSees Laboratory.

Newmark, N.M. & Rosenblueth, E. (1971). *Fundamentals of Earthquake Engineering*, Englewood Cliffs, N.J., USA, Prentice-Hall.

Seismosoft (2010). *SeismoStruct, A Computer Program for Static and Dynamic Nonlinear Analysis of Framed Structures*, URL: www.seismosoft.com.